Polymer Chemistry

PAPER

View Article Online
View Journal | View Issue

Cite this: *Polym. Chem.*, 2017, **8**, 5091

Norbornene-modified poly(glycerol sebacate) as a photocurable and biodegradable elastomer†

Yi-Cheun Yeh,[a] Liliang Ouyang,[a,b] Christopher B. Highley[a] and Jason A. Burdick *[a]

Received 26th February 2017,
Accepted 27th March 2017

DOI: 10.1039/c7py00323d

rsc.li/polymers

Poly(glycerol sebacate) (PGS) is a biodegradable elastomer that has emerged as a promising material in biomedical applications; however, the traditional thermal crosslinking of PGS limits its processing in the fabrication of three-dimensional (3D) scaffolds. Here, we designed a new photocurable PGS that uses thiol–ene click chemistry to control PGS crosslinking. Specifically, norbornene-functionalized PGS (Nor-PGS) macromers were crosslinked by varied amounts of a 4-arm thiolated crosslinker to program properties such as mechanics and degradation. The Nor-PGS crosslinked rapidly (<1 min to plateau modulus) under ultraviolet light and the storage modulus was dependent on the crosslinker amount, with a maximum storage modulus observed with an equimolar norbornene/thiol ratio. Tensile properties of Nor-PGS were also altered by the crosslinker concentration, with a simultaneous increase in elastic modulus and failure stress and decrease in elongation (ranging from ~170–240%) with higher crosslinker concentrations. In turn, the degradation of Nor-PGS was faster with lower crosslinker concentrations. To illustrate the processing of Nor-PGS, porous scaffolds with a range of sizes and shapes were fabricated using extrusion-based 3D printing, where the viscous macromer was extruded and crosslinked with continuous ultraviolet light exposure. Printed scaffolds supported the culture and proliferation of fibroblasts. These results indicate that crosslinked Nor-PGS is a promising functional elastomer for the fabrication of property-controllable scaffolds for biomedical applications.

Introduction

Poly(glycerol sebacate) (PGS), a thermally-crosslinked polyester, has great potential in tissue engineering due to its elasticity, biodegradability and cytocompatibility.[1–3] PGS is prepared through a polycondensation reaction of glycerol and sebacic acid, where the mechanical properties and degradation kinetics of PGS can be tailored by varying the curing temperature and time to match the requirements of intended applications.[4,5] For biological studies, PGS provides a conducive surface for cell adhesion and growth.[6,7] PGS degrades in a controlled manner with degradation products that are well tolerated in biological systems.[1,8] Particularly, PGS possesses rubber-like elasticity that can sustain and recover from deformation to match the elastomeric properties of many soft tissues in the body.[9,10] With these unique properties and positive attributes, PGS is increasingly being studied as scaffolds in dynamic environments (*e.g.*, heart[11] and cartilage[12]) and for tissue engineering applications (*e.g.*, cardiac,[13,14] vascular,[15,16] neural[17] tissues).

For use in biomedical applications, such as in the fabrication of tissue engineering scaffolds or as injectable materials, PGS must undergo a controlled crosslinking reaction. However, the traditional crosslinking of PGS is restricted by the difficulties of curing PGS at high temperatures and under vacuum. To expand the processing capabilities of PGS beyond thermal crosslinking, additional chemical modifications can be used. Towards this, PGS has been functionalized with various reactive groups (*e.g.*, acrylates[18,19] and cinnamates[20]) to allow crosslinking at room temperature using light. Acrylated-PGS (Acr-PGS) undergoes a free-radical photoinitiated polymerization that crosslinks in the presence of a photoinitiator and corresponding light, whereas cinnamate-modified PGS (PGS-CinA) undergoes a photodimerization upon irradiation with ultraviolet light.

PGS formed from Acr-PGS exhibits tunable mechanical properties by controlling the degree of acrylate substitution and PGS molecular weight.[18,19] By exploiting the photocrosslinking mechanism, Acr-PGS has been processed through electrospinning to fabricate biodegradable fibrous scaffolds with diverse mechanics (~60 kPa to 1 MPa).[21] Towards complex structures, Acr-PGS has also been applied to generate macroporous tissue scaffolds (*i.e.*, ear and meniscus) through 3D

[a]*Department of Bioengineering, University of Pennsylvania, Philadelphia, Pennsylvania, USA. E-mail: burdick2@seas.upenn.edu*
[b]*Department of Mechanical Engineering, Tsinghua University, Beijing, People's Republic of China*

†Electronic supplementary information (ESI) available. See DOI: 10.1039/c7py00323d

printing.[22] PGS-CinA forms networks where the properties (*e.g.*, mechanics and degradation) are controlled through the degree of substitution.[20] Likewise, elastomers from PGS-CinA have been formed that are cytocompatible and can be processed using replica-molding techniques.[20] In addition, PGS-CinA has been utilized to generate mesoporous elastomeric matrices to release small molecules in a controlled manner.[23]

Here, we introduce a new approach to crosslink modified PGS with photoinitiated thiol–ene reactions, through the modification of PGS with norbornene moieties. The thiol–ene reaction is a stepwise reaction that occurs in a stoichiometric ratio[24] and is also less susceptible to oxygen inhibition than other photoinitiated reactions.[25] Thus, thiol–ene reactions are able to rapidly polymerize at lower concentrations of photoinitiator and under ambient conditions,[26] which may further broaden the processing techniques available. In particular, due to the oxygen tolerance, thiol–ene reactions are highly cytocompatible as they do not generate intracellular reactive oxygen species (ROS) that are usually observed in common radical polymerizations.[27,28] Additionally, the step-growth mechanism results in uniform and controlled networks,[29] which may be advantageous compared to the heterogeneous network structure from chain-growth polymerization. Finally, thiol–ene reactions can be conducted under cytocompatible doses of ultraviolet light (*e.g.*, 10 mW cm^{-2}), providing an advantage over the cinnamate-based photocrosslinking that requires high energy input (*e.g.*, intense ultraviolet light (>100 mW cm^{-2}) or long exposure time (~2–3 h)) to achieve effective dimerization.[20,23,30,31]

Norbornene-functionalized PGS (Nor-PGS) is crosslinked by thiolated molecules in the presence of light and photoinitiator. The mechanical properties and degradation rates of Nor-PGS can be fine-tuned through changes in the amount of crosslinker, enabling the rational design of desired properties for specific applications. We applied the photocrosslinking of Nor-PGS macromers and thiolated crosslinkers for the fabrication of macroporous scaffolds using extrusion-based 3D printing and investigated their cytocompatibility with fibroblasts towards utility in tissue engineering.

Experimental

Materials

All chemicals were purchased from Sigma-Aldrich and used as received unless otherwise indicated.

Synthesis and characterization of PGS prepolymer and Nor-PGS

PGS prepolymer was synthesized *via* the condensation reaction of equimolar amounts of glycerol (Thermo Fisher Scientific) and sebacic acid.[1] The reagents were mixed and purged with N_2 for 10 min before heating. The mixture was stirred at 120 °C under N_2 flow for 2 h and then a vacuum of 12 mbar was applied for 46 h to obtain PGS prepolymer (Fig. 1a, top).

5-Norbornene-2-carbonyl chloride was prepared by reacting a mixture of 5-norbornene-2-carboxylic acid (0.58 ml, 4.75 mmol, a mixture of *endo*- and *exo*-, predominantly *endo*), oxalyl chloride (0.6 ml, 7.13 mmol) and dimethylformamide (DMF, 75 μl, Thermo Fisher Scientific), where DMF was used as a catalyst. These reagents were mixed and stirred in anhydrous dichloromethane (DCM, 10 ml, Thermo Fisher Scientific) at room temperature for 6 h under N_2. The excess oxalyl chloride and solvent were removed under reduced pressure. 5-Norbornene-2-carbonyl chloride was re-dissolved in anhydrous DCM and directly used for the functionalization of PGS.

PGS prepolymer (5 g) was dissolved in anhydrous DCM (60 ml) containing 500 ppm 4-methoxyphenol and 0.1 wt% 4-(dimethylamino)pyridine (DMAP). The reaction flask was cooled to 0 °C and the solution was purged with N_2 for 10 min. 5-Norbornene-2-carbonyl chloride (4.75 mmol in 7 ml DCM) was added dropwise into the PGS solution parallel to triethylamine (1 ml, 7.13 mmol) and then stirred at room temperature overnight (Fig. 1a, bottom). An additional 500 ppm 4-methoxyphenol was added to the reaction solution and DCM was removed using a rotary evaporator. Ethyl acetate was used to dissolve the remaining viscous liquid and the solution was vacuum filtered to remove triethylamine salts. Ethyl acetate was removed using a rotary evaporator to leave a viscous liquid. The viscous liquid was then dissolved in DCM and washed with hydrochloric acid (10 mM, three times), water (two times), and dried with anhydrous magnesium sulfate. After filtration of magnesium sulfate, DCM was removed *via* rotovapping to leave a viscous liquid, which was further dried in an oven (37 °C) overnight, and then purged with N_2 and stored at −20 °C. The norbornene modification of Nor-PGS was ~15% (calculation was based on the NMR analysis as described below) and the yield of Nor-PGS was ~96% (4.8 g as final product). To alter the norbornene modification on Nor-PGS, the PGS prepolymer was changed to 6.5 g and 3.5 g for 11% and 19% modification, respectively.

The chemical structures of PGS prepolymer and Nor-PGS macromers were verified using ^{1}H nuclear magnetic resonance (^{1}H NMR, Bruker Advance 360 MHz, Bruker). The chemical composition was majorly determined by calculating the signal integrals of –COC$\underline{H}_2$C$\underline{H}_2$C$\underline{H}_2$– at 1.31, 1.69–1.55, and 2.41–2.27 ppm for sebacic acid, –C$\underline{H}_2$C$\underline{H}$– at 3.5–5.2 ppm for glycerol, and –C$\underline{H}$=C$\underline{H}$– at 6.26–5.88 ppm for the vinyl protons on the norbornene groups. The signal intensity of the methylene groups of sebacic acid (1.69–1.55 ppm) and the vinyl protons on the norbornene groups (signal intensities of 6.26–5.88 ppm) were used to calculate the extent of norbornene modification. In detail, the signal intensity of the methylene groups of sebacic acid was normalized to 4, and the signal intensity of vinyl protons on the norbornene groups was divided by 2 to determine the percentage of norbornene on Nor-PGS.

The peak assignments in the NMR spectra for Nor-PGS macromers (15% norbornene modification) are listed below. ^{1}H NMR (360 MHz, $CDCl_3$) δ/ppm: 1.31 (52H, s, –C$\underline{H}_2$–),

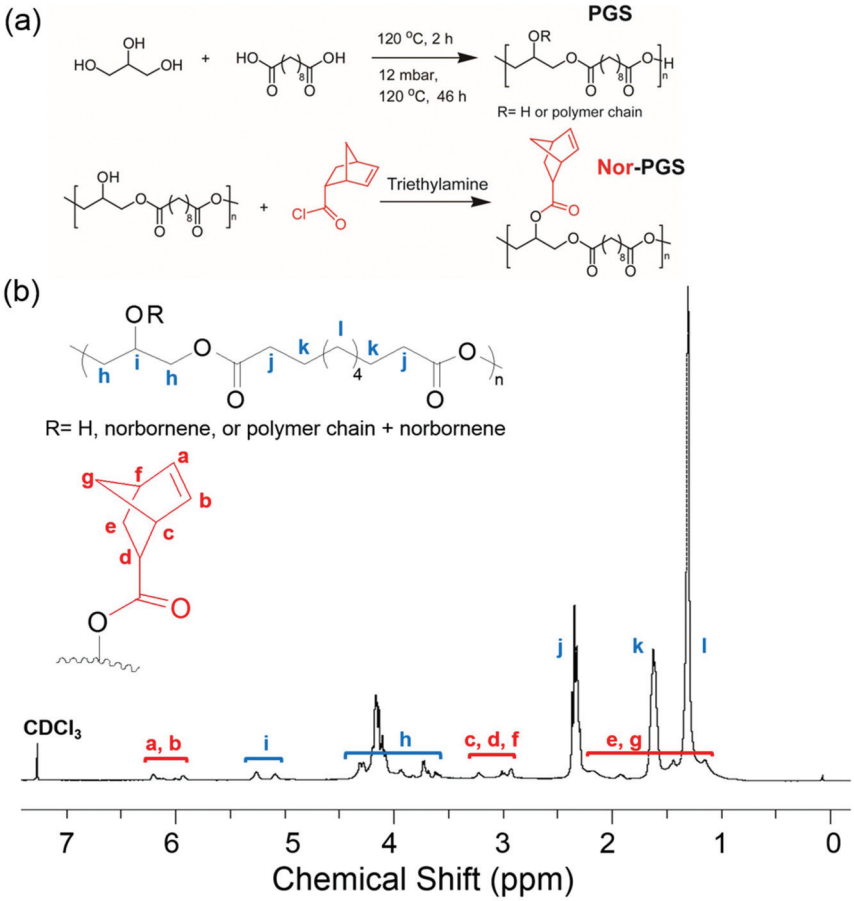

Fig. 1 (a) Synthesis scheme of PGS and Nor-PGS, with the synthesis of Nor-PGS from PGS through the coupling of 5-norbornene-2-carbonyl chloride to hydroxyl groups on PGS. (b) ^{1}H NMR spectrum of Nor-PGS.

1.51–1.23 ppm (2H, m, bridgehead proton and ring protons on the norbornene), 1.69–1.55 (26H, d, –C$\underline{H}_2$CH_2O(CO)–), 2.23–1.86 ppm (2H, m, bridgehead proton and ring protons on the norbornene), 2.41–2.27 (26H, m, –C$\underline{H}_2$O(CO)–), 3.30–2.90 (3H, m, bridge and α protons on the norbornene), 3.50–5.32 (36H, m, ORC$\underline{H}_2$C$\underline{H}$O–, R = H, norbornene or polymer chain + norbornene), 6.26–5.88 (2H, m, vinyl protons on the norbornene).

The molecular weight of the PGS prepolymer was measured using gel permeation chromatography (GPC). PGS prepolymer was dissolved in tetrahydrofuran (THF) at a concentration of 5 mg mL^{-1}. GPC-RI analyses were performed in THF (1.0 mL min^{-1}, 30 °C) using a Viscotek GPCmax with a VE 2001 GPC solvent/sample module, a 2600 UV-PDA detector, and a TDA 305 triple detector array. A set of two columns, including one PLgel 5 μm mixed-D and one PLgel 5 μm mixed-C columns, was used for separation and poly(methyl methacrylate) EasiVials standards (Agilent Technologies) were used for calibration.

Rheological measurement

Nor-PGS macromers were mixed with pentaerythritol tetrakis (3-mercaptopropionate) (PETMP) and 2,2-dimethoxy-2-phenyl-acetophenone (DMPA, 0.1 wt%) for crosslinking. Dynamic oscillatory time sweeps were performed using an AR2000 stress-controlled rheometer (TA Instruments) with an ultraviolet light-guide accessory (SmartSwap™, TA Instruments) connected to an ultraviolet light source (Omnicure S1000, EXFO). The photocrosslinking of Nor-PGS was carried out under exposure to ultraviolet light (365 nm, 10 mW cm^{-2}). Storage (G') and loss (G'') moduli with time were monitored under 0.5% strain and 1 Hz, using a cone and plate geometry (59 min 42 s (0.995°) cone angle, 20 mm diameter, 27 μm gap) at 25 °C.

Tensile testing

Photocured Nor-PGS samples with varied thiol/norbornene ratios (N = 0.5, 0.75 and 1) were prepared as dog-bone shaped specimens (~1 mm height, overall length of 30 mm, and a narrowed section that was 10 mm long and 5 mm wide). Samples were loaded into textured grips on an Instron 5848 universal testing system (Instron Corp., 5 N load cell) and tested with a 0.01 N preload and uniaxial extension (10 mm min^{-1}) until failure. Force and displacement data were acquired during loading and analyzed computationally (MATLAB, MathWorks) to determine sample stresses (calculated as measured forces

divided by cross-sectional areas), failure stresses (the maximum stresses achieved), failure strains (the strains at which the failure stresses were achieved), and elastic moduli (measured as the slopes from 40% to 50% strains). Cyclical loading test of Nor-PGS sample (N = 1) was performed at a jog rate of 60 mm min^{-1} in the elongation range of 30%–60% during 50 consecutive cycles.

Degradation behavior

For degradation analysis, Nor-PGS polymer disks (1 mm thick, 2 mm diameter) were prepared with different thiol/norbornene ratios (N = 0.5, 0.75 and 1) as described above. PGS disks were weighed, incubated in 1.5 ml of phosphate-buffered saline (PBS, pH 7.4), and placed on an orbital shaker at 37 °C. The solution was replaced with fresh PBS weekly. At each time point, three samples of each scaffold type were removed, lyophilized (Freezone 4.5, Labconco), and weighed to determine mass loss.

3D printing and imaging

Printing used a 3D printer adapted for deposition of materials by extrusion, which was described previously.[22,32,33] 3D structures (cube, nose and ear) were printed from respective 3D computer-aided design (CAD) models. Nor-PGS macromers, PETMP (thiol/norbornene = 1) and DMPA (0.1 wt%) were mixed in DCM and dried in oven (37 °C) overnight before printing. The materials were loaded into glass syringes (Gastight syringes, Hamiliton Company) with affixed blunt tip 25 G needles that were 6 mm long. Syringes were loaded onto the 3D printer and the printing was performed at ambient temperature (approximately 23 °C) with continuous irradiation of the print area with ultraviolet light (365 nm, 10 mW cm^{-2}) during printing and for five minutes post-printing. Printed PGS scaffolds were imaged using scanning electron microscopy (SEM, FEI Quanta 600 environmental scanning electron microscope).

Cell culture and characterization of cell-seeded PGS scaffolds

NIH 3T3 fibroblast cells (ATCC) were cultured at 37 °C under a humidified atmosphere of 5% CO_2 in high glucose Dulbecco's Modified Eagle's Medium (DMEM, 4.5 g L^{-1} glucose) containing 10% fetal bovine serum (FBS) and 1% penicillin/streptomycin. For cell seeding, 3D-printed PGS scaffolds were sterilized by incubation in 70% ethanol for 30 min, washed with PBS, and incubated in serum-contained media for 24 h. As an initial test of cell adhesion and viability, 3T3 cell suspensions (1×10^6 cells in 2 ml) were added onto 3D printed PGS scaffolds (2-layer, 10 × 10 mm, height: 0.16 mm) in a cell culture dish (diameter × height, 35 mm × 10 mm). After 24 h, the cell-seeded scaffolds were transferred to a new cell culture dish and stained with calcein-AM (2 μM in PBS, Life Technologies) at room temperature for 20 min before imaging. Fluorescent images were taken using an Olympus BX51 microscope (B&B Microscopes Limited).

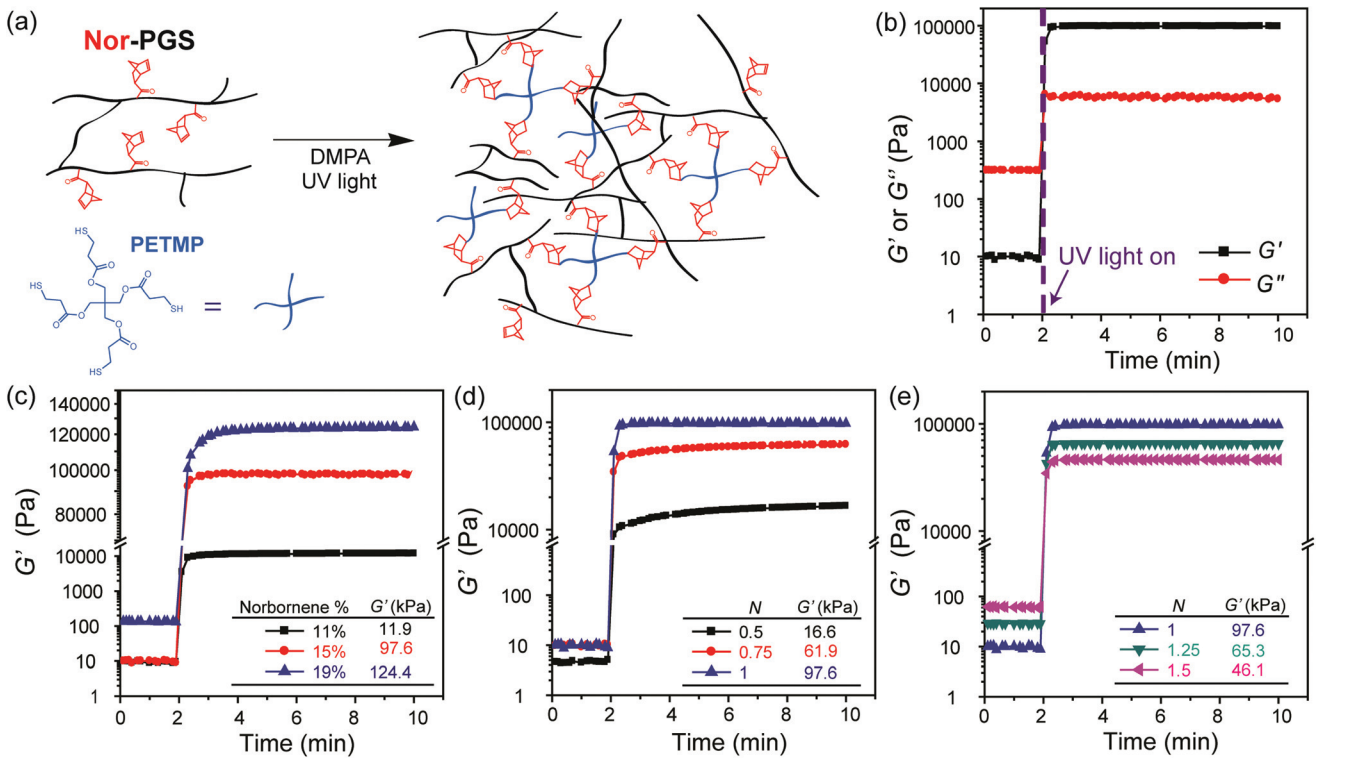

Fig. 2 (a) Scheme of Nor-PGS crosslinking through the light initiated thiol–norbornene reaction between Nor-PGS and PETMP. (b) Rheology of the photocrosslinking of Nor-PGS in the presence of PETMP and ultraviolet light (365 nm, 10 mW cm^{-2}). The storage moduli (G') of Nor-PGS networks were varied through (c) the extent of norbornene modification (11, 15, 19% with thiol/norbornene = 1) and (d, e) thiol/norbornene ratio (N) with 15% norbornene modified Nor-PGS.

To assess cell proliferation, 3T3 cell suspensions (1×10^5 cells in 100 μl) were seeded onto 3D printed PGS scaffolds (10-layer, 10 × 10 mm, height: 0.8 mm) in a 24-well cell culture plate. The scaffolds were incubated for 2 h and then 2 ml of culture medium was added. After 24 h, the scaffolds were transferred to a non-tissue culture treated 12-well plate and assessed for metabolic activity for up to 8 days using an Alamar blue assay according to the manufacturer's protocol (Invitrogen Biosource, USA).

Statistical analysis

One-way analysis of variance (ANOVA) was performed on data sets to determine statistical significance of differences in mechanical testing, degradation and cell activity. Significance was set at $p < 0.05$ with *, ** or *** indicating $p < 0.05$, 0.01 or 0.001, respectively. Error bars are reported in figures as the standard deviation (s.d.) unless otherwise noted.

Results and discussion

PGS is an elastic, biocompatible and biodegradable polymer increasingly used in a variety of biomedical applications. Functionalization of PGS, such as by acrylation,[18,19] has been used to process PGS into complex, multi-scale structures. Here, we implemented a new modification (*i.e.*, norbornene) of PGS to allow the processing of PGS *via* thiol–ene crosslinking, to impart features such as rapid polymerization, oxygen insensitivity, orthogonal reaction between thiols and norbornenes, and controllable crosslinking. This modification may further expand the processing capability of PGS and provide a simple technique to tune PGS properties.

PGS prepolymer was synthesized *via* a polycondensation reaction of glycerol and sebacic acid in a 1 : 1 molar ratio and a weight average molecular weight (M_w) of 7.06 kDa with polydispersity index of 5.06 was obtained *via* reaction for 46 h at 120 °C (Fig. 1a, top). Hydroxyl groups of PGS were then reacted with 5-norbornene-2-carbonyl chloride to obtain norbornene-functionalized PGS (Nor-PGS) (Fig. 1a, bottom). The incorporation of norbornene groups to the PGS prepolymer (11–19% modification) was confirmed in ^{1}H NMR by the appearance of peaks at δ 6.26–5.88 ppm for the vinyl protons on the norbornene groups (Fig. 1b).

The crosslinking of Nor-PGS was investigated using photorheology. The norbornenes on Nor-PGS macromers undergo a thiol–ene reaction with thiols on the four-arm thiolated cross-

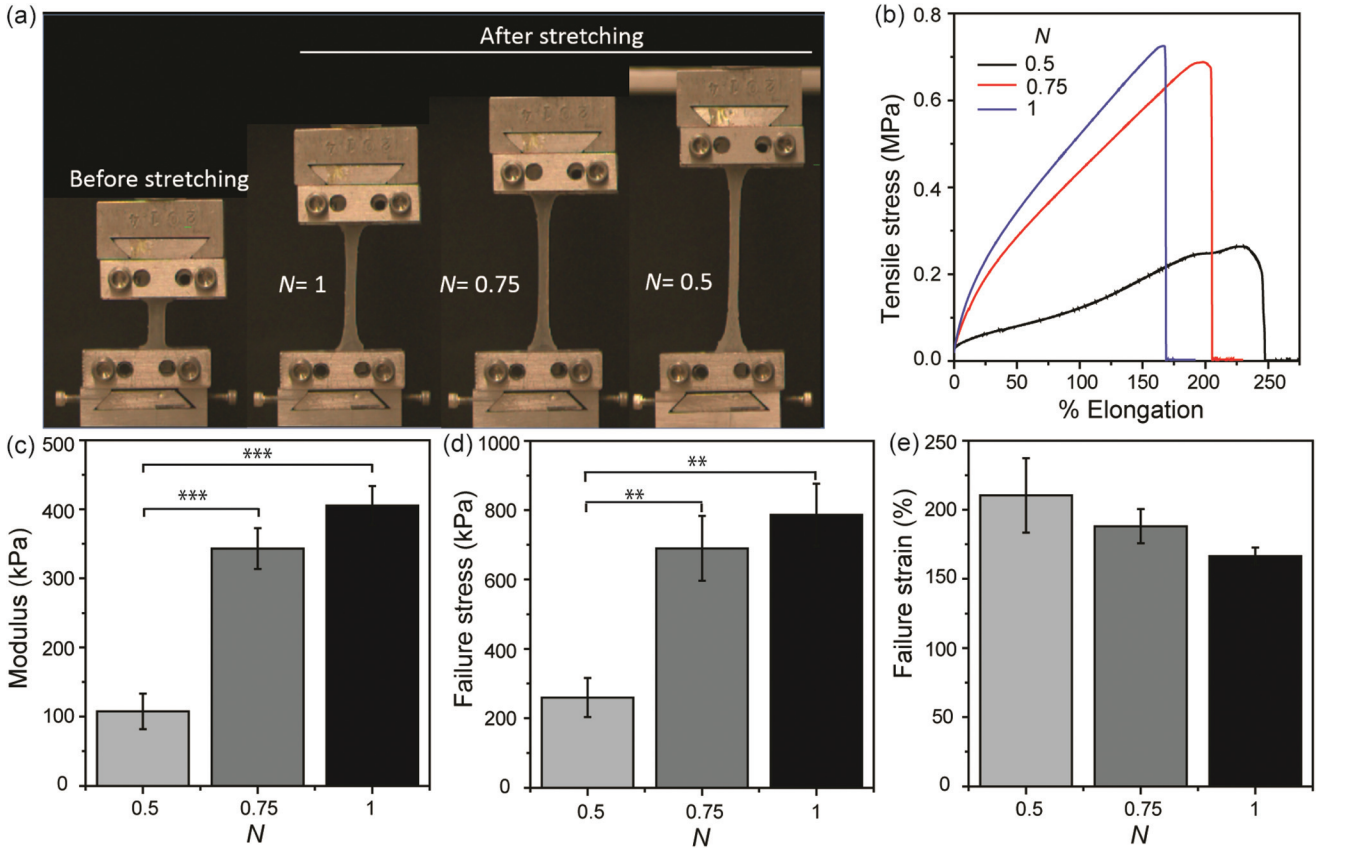

Fig. 3 (a) Representative images of Nor-PGS samples with varied thiol/norbornene ratios (*N*) before and after (images taken immediately before failure) tensile loading. (b) Representative tensile stress *versus* elongation profiles for networks formed from the Nor-PGS macromers with varied thiol/norbornene ratios. (c) Modulus, (d) failure stress, and (e) failure strain of the Nor-PGS samples with varied thiol/norbornene ratios. n = 3 measurements per group, data presented as mean ± s.d., $^{**}p < 0.01$ and $^{***}p < 0.001$.

linker PETMP in the presence of the photoinitiator DMPA (0.1 wt%) and ultraviolet light (365 nm, 10 mW cm^{-2}) (Fig. 2a). Nor-PGS macromers were crosslinked by PETMP rapidly as the crossover of the storage (G') and the loss (G'') moduli occurred in seconds, and G' increased multiple orders of magnitude and reached a plateau within one minute of light exposure (Fig. 2b). The rheological properties of Nor-PGS networks can be altered through the extent of norbornene modification of the Nor-PGS macromers or through the thiol/norbornene ratio (N). The G' at the plateau increased with increasing norbornene modification in Nor-PGS, ~12, 98, and 124 kPa for 11, 15, and 19% Nor-PGS modification, respectively (Fig. 2c). Using the same Nor-PGS (15% norbornene modification), the plateau G' was controlled with the concentration of PETMP due to varied extents of crosslinking and ranged from ~17 to 98 kPa (Fig. 2d and e). The maximum G' was observed at a thiol/norbornene ratio equal to 1 as each thiol was able to react with a norbornene to make an effective crosslink. With a thiol/norbornene ratio greater than one, the G' dropped from the maximum value due to saturation of norbornene groups and excess thiols, yielding networks with free pendant thiols.

Additional mechanical properties of Nor-PGS networks were determined with tensile testing. Nor-PGS samples were prepared with varied thiol/norbornene ratios (N = 0.5, 0.75 and 1) to vary the extent of crosslinking. The % elongation of Nor-PGS was modulated by the PETMP amount used for photocrosslinking, showing ~170, 200, and 240% elongation for thiol/norbornene ratios of 1, 0.75, and 0.5, respectively (Fig. 3a and b). The measured properties of the Nor-PGS samples also varied with PETMP amount. The highest elastic modulus of ~400 kPa was observed for the Nor-PGS with N = 1, followed by the N = 0.75 at ~340 kPa, and N = 0.5 at ~110 kPa (Fig. 3c). Failure stresses presented a similar trend, with N = 1 failing at ~790 kPa, N = 0.75 at ~690 kPa, and N = 0.5 at ~260 kPa (Fig. 3d). Failure strains followed an opposite trend, and were measured at ~170% for N = 1, ~190% for N = 0.75, and ~210% for N = 0.5 (Fig. 3e). All Nor-PGS samples exhibited elastic properties, and their tensile properties were easily tuned by changing the crosslinker amount. Increased crosslinker amount, up to N = 1, resulted in a higher extent of crosslinking, presenting stronger mechanical properties of the Nor-PGS network, while decreased crosslinker amounts resulted in the formation of a soft Nor-PGS network with high elongation of over 200%. In addition, the hysteresis test of Nor-PGS (N = 1) was performed in the elongation range of 30%–60%, showing that the Nor-PGS elastomer maintained its tensile property with minimal creep deformation after 50 tensile cycles (Fig. 4).

Previous studies have reported that PGS[22,34,35] and the thiolated crosslinker PETMP[36] present hydrolytic degradability due to the ester moieties in their structures. Here, degradation of Nor-PGS was investigated in PBS (pH 7.4) at 37 °C (Fig. 5). Mass loss of the N = 0.5 sample was greater than the N = 0.75 and N = 1 groups, indicating that decreased crosslinking in Nor-PGS results in faster degradation. This control over degradation properties in Nor-PGS by varying crosslinker amounts would be useful to shorten or extend the lifetime of the Nor-PGS scaffolds depending on the application.

The processing of Nor-PGS into scaffolds was demonstrated using 3D printing. We applied Nor-PGS as a photocurable ink for 3D printing to fabricate porous structures through the extrusion of material in a layer-by-layer deposition process. Mixtures of Nor-PGS macromers, PETMP crosslinkers and

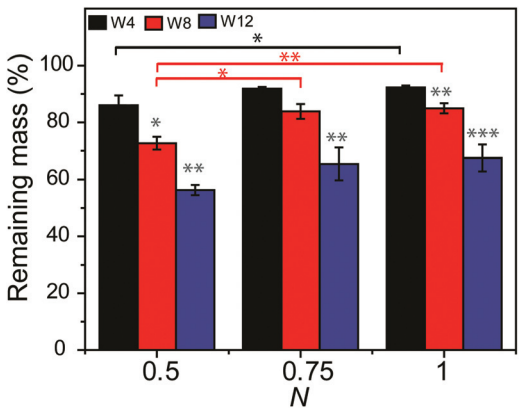

Fig. 5 Nor-PGS degradation in PBS (pH 7.4) at 37 °C. In each Nor-PGS (N = 0.5, 0.75 and 1) group, the statistical significance (denoted in gray asterisk) was calculated based on the samples of week 8 (W8) and week 12 (W12) relative to the sample of week 4 (W4). For comparison between groups, the statistical significance is denoted in black and red asterisk. n = 3 measurements per group, data presented as mean ± s.d., *p < 0.05, **p < 0.01 and ***p < 0.001.

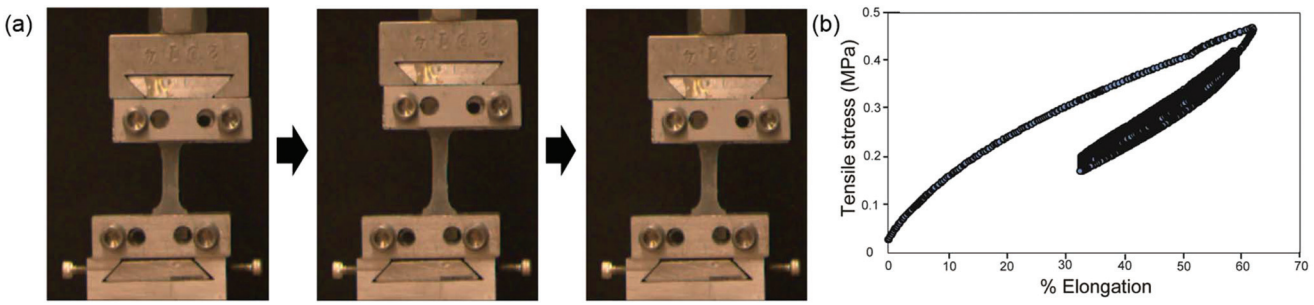

Fig. 4 (a) Representative images and (b) tensile stress–elongation profile of Nor-PGS (N = 1) during 50 cycles of tensile loading.

DMPA photoinitiator were prepared as inks to print designed constructs, where the materials were extruded from a syringe on a standard 3D printer and cured by continuous exposure to ultraviolet light (365 nm, 10 mW cm^{-2}) upon extrusion. A typical multi-layer lattice cube structure was printed with good integrity (65 layers with 8 × 8 mm in cross-section and 5 mm in height), demonstrating the general printability of Nor-PGS (Fig. 6a). The open-lattice cube structure was imaged using SEM to illustrate its porous structure and uniform printed filaments (Fig. 6b). In addition, heteromorphic structures were also printed to further illustrate printability, including a human nose and ear of ~30 mm in length (Fig. 6c and d). The printed Nor-PGS structures were elastic, as the ear can be deformed under an applied force and returned

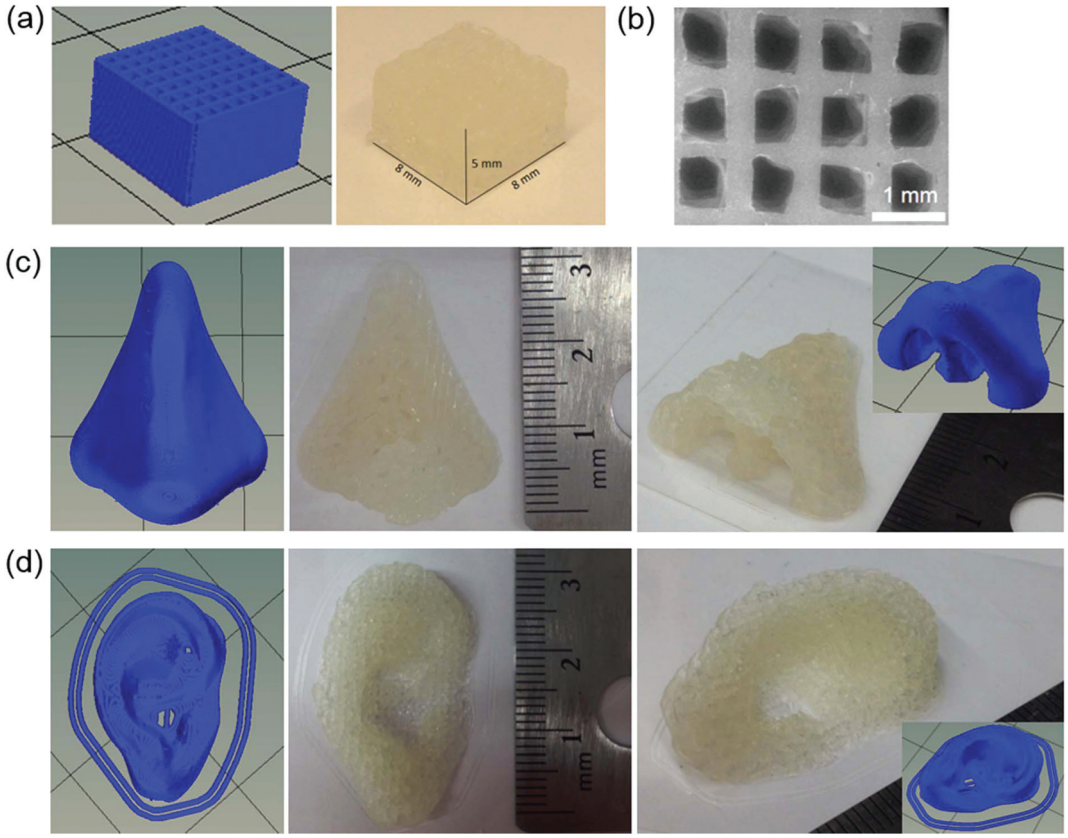

Fig. 6 (a) 3D printed Nor-PGS lattice cube structure and (b) SEM image. The lattice structure was printed up to 65 layers with 8 × 8 mm in cross-section, 5 mm in height, and 1 mm for the gap between filaments. Computer designs and printed cartilaginous structures of (c) a nose and (d) an ear.

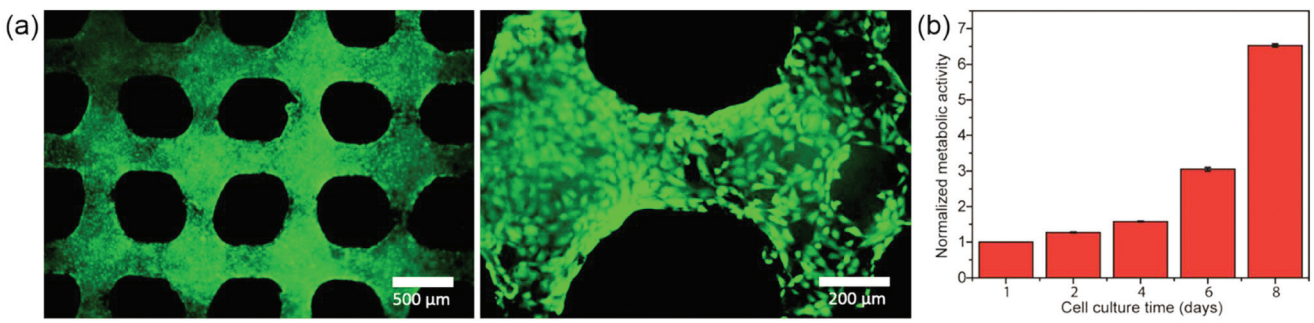

Fig. 7 (a) 3T3 fibroblasts cultured on a 2-layered scaffold and stained with calcein-AM after culture for 24 h. (b) Normalized (to day 1 values) metabolic activity of 3T3 fibroblasts on a 10-layered scaffold, where activity was determined for up to 8 days using an Alamar blue assay. n = 3 measurements per group, data presented as mean ± s.d., values at all time points were statistically significant from each other ($p < 0.001$).

to its geometry on removal of that force (Movie S1†). These results demonstrate that Nor-PGS is a promising material to fabricate complex elastomeric scaffolds through 3D printing.

To demonstrate the cytocompatibility of crosslinked Nor-PGS, NIH 3T3 fibroblasts were seeded throughout 3D printed scaffolds. Cell attachment and proliferation were investigated using calcein AM staining and metabolic assays, respectively. The fibroblasts were viable and spread into dense layers (Fig. 7a), which was expected based on previously reported observations of cellular adhesion to PGS surfaces.[1,2] Cellular metabolism, a means of assessing proliferation, was monitored using an Alamar blue assay, where fluorescence resulting from enzymatic activity on a fluorogenic substrate was measured. The cellular metabolism of cells on the 3D printed Nor-PGS constructs increased over time (Fig. 7b). These results demonstrate that the thiol–norbornene reaction within the PGS network as well as the 3D printing process did not alter the inherent cytocompatibility of PGS.

Conclusion

We developed a reactive norbornene functionalization of PGS that facilitates its crosslinking using a thiol–ene reaction and processing through techniques such as 3D printing. Nor-PGS networks exhibit tunable mechanical properties and degradation rates in the presence of different concentrations of crosslinker, allowing the use of the same functionalized Nor-PGS to obtain networks with varied properties that can be tuned to a specific application. We also demonstrated the utility of Nor-PGS in the fabrication of 3D-printed scaffolds that supported the attachment and proliferation of cells. Taken together, we synthesized a new functionalized PGS, where the robustness of the thiol–norbornene photochemistry can be used to fabricate elastomeric, biodegradable and cytocompatible scaffolds for biomedical applications.

Acknowledgements

This work was supported by an American Heart Association Established Investigator Award and a National Science Foundation MRSEC Award. L. O. acknowledges financial support from the China Scholarship Council (L. O. File 201506210148).

References

1 Y. Wang, G. Ameer, H. Sheppard and R. Langer, *Nat. Biotechnol.*, 2002, **20**, 602–606.
2 X. J. Loh, A. A. Karim and C. Owh, *J. Mater. Chem. B*, 2015, **3**, 7641–7752.
3 R. Rai, M. Tallawi, A. Grigore and A. R. Boccaccini, *Prog. Polym. Sci.*, 2012, **37**, 1051–1078.
4 I. Jaafar, M. Ammar, S. Jedlicka, R. Pearson and J. Coulter, *J. Mater. Sci.*, 2010, **45**, 2525–2529.
5 X. Li, A. T.-L. Hong, N. Naskar and H.-J. Chung, *Biomacromolecules*, 2015, **16**, 1525–1533.
6 J. Gao, A. E. Ensley, R. M. Nerem and Y. Wang, *J. Biomed. Mater. Res., Part A*, 2007, **83**, 1070–1075.
7 S. Redenti, W. L. Neeley, S. Rompani, S. Saigal, J. Yang, H. Klassen, R. Langer and M. J. Young, *Biomaterials*, 2009, **30**, 3405–3414.
8 Y. Wang, Y. M. Kim and R. Langer, *J. Biomed. Mater. Res., Part A*, 2003, **66**, 192–197.
9 M. J. N. Pereira, B. Ouyang, C. A. Sundback, N. Lang, I. Friehs, S. Mureli, I. Pomerantseva, J. McFadden, M. C. Mochel, O. Mwizerwa, P. Nido, D. Sarkar, P. T. Masiakos, R. Langer, L. S. Ferreira and J. M. Karp, *Adv. Mater.*, 2013, **25**, 1209–1215.
10 M. J. Kim, M. Y. Hwang, J. H. Kim and D. J. Chung, *BioMed Res. Int.*, 2014, 956952.
11 Q. Z. Chen, A. Bismarck, U. Hansen, S. Junaid, M. Q. Tran, S. E. Harding, N. N. Ali and A. R. Boccaccini, *Biomaterials*, 2008, **29**, 47–57.
12 J. M. Kemppainen and S. J. Hollister, *J. Biomed. Mater. Res., Part A*, 2010, **94**, 9–18.
13 Q.-Z. Chen, H. Ishii, G. A. Thouas, A. R. Lyon, J. S. Wright, J. J. Blaker, W. Chrzanowski, A. R. Boccaccini, N. N. Ali, J. C. Knowles and S. E. Harding, *Biomaterials*, 2010, **31**, 3885–3893.
14 G. C. Engelmayr Jr., M. Cheng, C. J. Bettinger, J. T. Borenstein, R. Langer and L. E. Freed, *Nat. Mater.*, 2008, **7**, 1003–1010.
15 D. Motlagh, J. Yang, K. Y. Lui, A. R. Webb and G. A. Ameer, *Biomaterials*, 2006, **27**, 4315–4324.
16 C. J. Bettinger, E. J. Weinberg, K. M. Kulig, J. P. Vacanti, Y. D. Wang, J. T. Borenstein and R. Langer, *Adv. Mater.*, 2006, **18**, 165–169.
17 C. A. Sundback, J. Y. Shyu, Y. Wang, W. C. Faquin, R. S. Langer, J. P. Vacanti and T. A. Hadlock, *Biomaterials*, 2005, **26**, 5454–5464.
18 C. L. E. Nijst, J. P. Bruggeman, J. M. Karp, L. Ferreira, A. Zumbuehl, C. J. Bettinger and R. Langer, *Biomacromolecules*, 2007, **8**, 3067–3073.
19 J. L. Ifkovits, R. F. Padera and J. A. Burdick, *Biomed. Mater.*, 2008, **3**, 034104.
20 C. Zhu, S. R. Kustra and C. J. Bettinger, *Acta Biomater.*, 2013, **9**, 7362–7370.
21 J. L. Ifkovits, J. J. Devlin, G. Eng, T. P. Martens, G. Vunjak-Novakovic and J. A. Burdick, *Appl. Mater. Interfaces*, 2009, **1**, 1878–1886.
22 Y.-C. Yeh, C. B. Highley, L. Ouyang and J. A. Burdick, *Biofabrication*, 2016, **8**, 045004.
23 P. Pholpabu, S. S. Yerneni, C. Zhu, P. G. Campbell and C. J. Bettinger, *ACS Biomater. Sci. Eng.*, 2016, **2**, 1464–1470.
24 B. D. Fairbanks, M. P. Schwartz, A. E. Halevi, C. R. Nuttelman, C. N. Bowman and K. S. Anseth, *Adv. Mater.*, 2009, **21**, 5005–5010.
25 S. C. Ligon, B. Husar, H. Wutzel, R. Holman and R. Liska, *Chem. Rev.*, 2014, **114**, 557–589.

26 J. D. McCall and K. S. Anseth, *Biomacromolecules*, 2012, **13**, 2410–2417.
27 A. D. Shubin, T. J. Felong, D. Graunke, C. E. Ovitt and D. S. W. Benoit, *Tissue Eng., Part A*, 2015, **21**, 1733–1751.
28 J. J. Roberts and S. J. Bryant, *Biomaterials*, 2013, **34**, 9969–9979.
29 G. Odian, *Principles of Polymerization*, Wiley, New York, 1991.
30 P. Gupta, S. R. Trenor, T. E. Long and G. L. Wilkes, *Macromolecules*, 2004, **37**, 9211–9218.
31 F. M. Andreopoulos, C. R. Deible, M. T. Stauffer, S. G. Weber, W. R. Wagner, E. J. Beckman and A. J. Russell, *J. Am. Chem. Soc.*, 1996, **118**, 6235–6240.
32 C. B. Highley, C. B. Rodell and J. A. Burdick, *Adv. Mater.*, 2015, **27**, 5075–5079.
33 L. Ouyang, C. B. Highley, C. B. Rodell, W. Sun and J. A. Burdick, *ACS Biomater. Sci. Eng.*, 2016, **2**, 1743–1751.
34 X. Li, A. T. L. Hong, N. Naskar and H.-J. Chung, *Biomacromolecules*, 2015, **16**, 1525–1533.
35 M. Frydrych and B. Chen, *J. Mater. Chem. B*, 2013, **1**, 6650–6661.
36 A. Oesterreicher, J. Wiener, M. Roth, A. Moser, R. Gmeiner, M. Edler, G. Pinter and T. Griesser, *Polym. Chem.*, 2016, **7**, 5169–5180.